D. Pliatsios, T. Lagkas, V. Argyriou, A. Sarigiannidis, D. Margounakis, T. Saoulidis, and P. Sarigiannidis, "A Hybrid RF-FSO Offloading Scheme for Autonomous Industrial Internet of Things," IEEE INFOCOM 2022 - IEEE Conference on Computer Communications Workshops (INFOCOM WKSHPS), Jun. 2022, pp. 1-6, doi: 10.1109/INFOCOMWKSHPS54753.2022.9798011.

A Hybrid RF-FSO Offloading Scheme for Autonomous Industrial Internet of Things

Dimitrios Pliatsios*, Thomas Lagkas†, Vasileios Argyriou‡, Antonios Sarigiannidis§,
Dimitrios Margounakis§, Theocharis Saoulidis§, and Panagiotis Sarigiannidis*
*Department of Electrical and Computer Engineering, University of Western Macedonia, 50100 Kozani, Greece
† Department of Computer Science, International Hellenic University, Kavala Campus, Greece
‡ Department of Networks and Digital Media, Kingston University, Kingston upon Thames, United Kingdom
§ Sidroco Holdings Ltd., 1077 Nicosia, Cyprus
dpliatsios@uowm.gr, tlagkas@ieee.org, vasileios.argyriou@kingston.ac.uk, asarigia@sidroco.com,
dmargoun@sidroco.com, hsaoulidis@sidroco.com, psarigiannidis@uowm.gr

***Abstract*—The ever increasing demand for bandwidth triggered by data-intensive applications is imposing a considerable burden on the radio-frequency (RF) spectrum. A promising solution to address the spectrum congestion problem is the adoption of free-space optical (FSO) communications. In this work, we consider a hybrid RF-FSO system that enables the task offloading process from Industrial Internet-of-Things devices to a multi-access edge computing (MEC)-enabled base station (BS). We propose a solution that minimizes the total energy consumption of the system by deciding whether the RF or FSO link will be used for the task offloading and optimally allocating the device transmission power while taking into account the task requirements in terms of delay. The proposed solution is based on a decomposition-driven algorithm that employs integer linear programming (ILP) and Lagrange dual decomposition. Finally, we carry out system-level Monte Carlo simulations to evaluate the performance of the solution. The simulation results show that the proposed solution can minimize the total energy consumption within a few iterations, while also considering the respective latency requirements.**

***Index Terms*—Computation Offloading, Energy Efficiency, Free-space Optical Communications, Industrial Internet of Things, Multi-access Edge Computing**

I. Introduction

Autonomous and intelligent internet-of-things (IoT) devices are becoming widely used in various domains such as healthcare, transportation, and industry. As a result, the emerging internet-of-everything (IoE) is expected to result in considerable increases in both the traffic volume and the number of connected devices [1]. Although the fifth-generation (5G) mobile networks offer significant improvements over the previous generations, they may not be able to satisfy the requirements of future emerging autonomous and intelligent systems [2]. To realize the IoE paradigm, future beyond-5G (B5G) and sixth-generation (6G) mobile networks have to address the limitations of current networks by integrating a wide range of novel technologies such as artificial intelligence, quantum communications, intelligent reflecting surfaces, terahertz and free-space optical communications (FSO) [3], [4].

Particularly, the adoption of FSO communications is a promising technology to address the congestion of the radio-frequency (RF) spectrum. FSO communications is a line-of-sight (LOS) technology that transmits data between two transceivers over small (e.g., indoor, building-to-building) or large (e.g., satellites) distances using visible or infrared light [5]. Moreover, the directional characteristic of the light beam employed in FSO enables spatial reuse and impedes eavesdropping, resulting in increased data privacy and security. Also, the use of light provides immunity to electromagnetic interference offering redundant communication links in disaster-recovery scenarios [6].

Motivated by the advantages offered by FSO communications, research efforts are being focused on integrating FSO communications in various applications. In particular, the authors in [7] developed a strategy to minimize the backhauling cost by choosing either a hybrid RF-FSO or optical communication system. Khan *et al.* [8] proposed a hybrid RF-FSO communication system and designed a power and modulation adaptive scheme for maximizing the power gain. Moreover, in [9], the authors developed a throughput maximization approach for a channel adaptive hybrid RF-FSO communication system. The authors in [10] designed a low-complexity suboptimal method to find the optimal trajectory of an unmanned aerial vehicle (UAV) that support wireless backhauling using FSO communications.

In addition, the authors in [11] designed a method for the joint optimization of fronthaul compression and RF time allocation in an uplink cloud-radio access network that consists of a hybrid RF-FSO fronthauling technology. A network architecture consisting of high altitude platforms equipped with FSO transceivers is presented in [12]. Also, the authors derived closed-form statistical channel models to simplify the optimal design of such systems. Bashir and Alouini [13] developed an approach to minimize the outage probability by optimizing the power allocation considering the noise power and pointing errors. In [14], the authors focused on maximizing the long-term capacity of a FSO system by developing a power optimization approach based on reinforcement learning.

In this work, we consider an industrial internet-of-things environment, where a number of autonomous and intelligent IIoT devices (e.g., robotics) are able to offload the AI processing to a MEC-enabled BS through a hybrid RF-FSO communication

system. We propose a solution that aims to minimize the total energy consumption of the system through the optimal selection between the RF or FSO link and the allocation of the transmission power, taking into account the latency requirements. In more detail, the technical contributions of this work are as follows:

- We present a hybrid RF-FSO system model that enables the offloading of IIoT tasks to a MEC-enabled BS.
- We formulate the minimization of the system energy consumption as a joint optimization of the RF-FSO link selection decision and the allocation of RF and FSO power. Moreover, we discuss the convexity of the original optimization problem.
- As the joint optimization problem is challenging to solve, we decouple the initial problem into two subproblems and solve each subproblem in an iterative way.
- In particular, the RF-FSO link decision subproblem is formulated as an integer linear programming (ILP) problem which is solved using the CVX toolbox with the Mosek solver. On the other hand, the Lagrange and subgradient methods are utilized for finding the optimal transmission power for the RF and FSO links, respectively.
- Finally, we evaluate the performance of the proposed approach through system-level Monte Carlo simulations in terms of total energy consumption.

The remainder of the paper is structured as follows: In Section II we discuss the model and the problem formulation, while, in Section III, we present the proposed solution. We provide the evaluation results in Section IV and we conclude the work in Section V.

II. System Model and Problem Formulation

Fig. 1 depicts the architecture of the considered system model. A number of IIoT devices are served by a BS with MEC capabilities. Each device is equipped with both RF and FSO transceivers, while the BS is equipped with RF and K FSO transceivers. Additionally, the BS have beam-tracking capabilities in order to minimize directional errors.

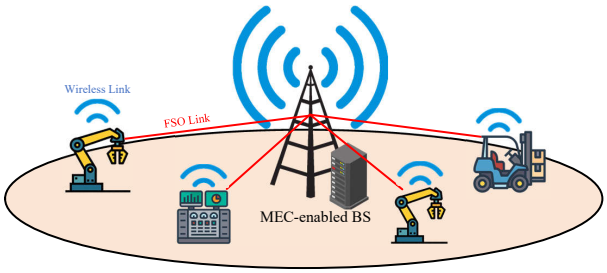

Fig. 1. Task Uploading in the Hybrid RF-FSO Offloading Scenario

Let N denote the number of IIoT devices that are served by the BS. We assume that each device has a single AI task to be processed by the MEC-enabled BS, thus, the terms device and task can be used interchangeably. The i-th AI task is described by the tuple (L_i, T_i^{max}), where L_i denotes the data size in bits to be processed and T_i^{max} denotes the maximum tolerable latency for the task upload.

A. RF Communication Model

The RF link capacity between a device and the BS is calculated by

$$R_i^{rf} = w_i^{rf} \log_2(1 + \frac{p_i^{rf}|h_i^{rf}|^2}{\sigma^2}) \tag{1}$$

where w_i^{rf} is the available RF bandwidth, p_i^{rf} is the RF transmission power, $|h_i^{rf}|^2$ denotes the channel gain consisting of distance-based pathloss and Rayleigh fading and σ^2 is the spectral power of the additive Gaussian white noise (AWGN).

B. FSO Communication Model

FSO links are highly directional, while the atmospheric effects have a considerable impact on the link quality [15].The FSO communication model adopted in this work considers the effects of both turbulence-induced fading and distance-based pathloss [16]. Therefore, the FSO link capacity between a device and the BS is calculated by

$$R_i^{fso} = w_i^{fso} \log_2(1 + \frac{p_i^{fso}|h_i^{fso}|^2}{\sigma^2}) \tag{2}$$

where w_i^{fso} is the FSO bandwidth, p_i^{fso} is the FSO transmission power, and $|h_i^{fso}|^2$ is the FSO channel gain that is obtained by

$$h_i^{fso} = h_i^l h_i^f \tag{3}$$

where h_i^f denotes the impact of atmospheric turbulence and can be modeled as a log-normal distribution. Moreover, h_i^l denotes the distance-based pathloss and is calculated as follows:

$$h_i^l = \frac{A_{TX} A_{RX} e^{-\alpha d_i}}{(\lambda d_i)^2} \tag{4}$$

In (4), A_{TX} and A_{RX} are the aperture areas of the transmitter and receiver, respectively, while α is a coefficient that depends on the environment and wavelength. Additionally, d_i is the distance between the device and the BS, while λ is the wavelength used for the transmission.

C. Problem Formulation

With respect to the RF link, the time required for transmitting the i-th task is calculated as

$$T_i^{rf} = \frac{L_i}{R_i^{rf}} \tag{8}$$

and the corresponding energy consumption is calculated by

$$E_i^{rf} = p_i^{rf} T_i^{rf} \tag{9}$$

On the other hand, with respect to the FSO link, the time required for transmitting the i-th task is calculated as

$$T_i^{fso} = \frac{L_i}{R_i^{fso}} \tag{10}$$

$$L = \sum_{i=1}^{N}[x_i E_i^{rf} + (1-x_i)E_i^{fso}] + \sum_{i=1}^{N}\tau_i[x_i T_i^{rf} + (1-x_i)T_i^{fso} - T_i^{max}] + \sum_{i=1}^{N}\pi_i[x_i p_i^{rf} + (1-x_i)p_i^{fso} - p_i^{max}] \quad (5)$$

$$\frac{\partial L}{\partial p_i^{rf}} = x_i \left[\pi_i + \frac{L_i \left(-\frac{h_i^{rf}(p_i^{rf}+\tau_i)}{N_0 + h_i^{rf} p_i^{rf} \ln 2} + \log_2 \left[1 + \frac{h_i^{rf} p_i^{rf}}{N_0} \right] \right)}{w_i^{rf} \log_2 \left[1 + \frac{h_i^{rf} p_i^{rf}}{N_0} \right]^2} \right] \quad (6)$$

$$\frac{\partial L}{\partial p_i^{fso}} = (1-x_i) \left[\pi_i - \frac{L_i \left(\frac{h_i^{fso}(p_i^{fso}+\tau_i)}{N_0 + h_i^{fso} p_i^{fso} \ln 2} - \log_2 \left[1 + \frac{h_i^{fso} p_i^{fso}}{N_0} \right] \right)}{w_i^{fso} \log_2 \left[1 + \frac{h_i^{fso} p_i^{fso}}{N_0} \right]^2} \right] \quad (7)$$

and the corresponding energy consumption is calculated by

$$E_i^{fso} = p_i^{fso} T_i^{fso} \quad (11)$$

We introduce variable x_i that denotes whether the RF (i.e., $x_i = 1$) or the FSO (i.e., $x_i = 0$) link will be used for the upload of the i-th task. Therefore, the time required for transmitting the i-th is obtained by

$$T_i(x_i, p_i^{rf}, p_i^{fso}) = x_i T_i^{rf} + (1-x_i)T_i^{fso} \quad (12)$$

while the total consumed energy is obtained by

$$E_i(x_i, p_i^{rf}, p_i^{fso}) = x_i E_i^{rf} + (1-x_i)E_i^{fso} \quad (13)$$

We aim to minimize the total power consumption of the system by optimizing the link decision. Consequently, the optimization problem is expressed as follows:

$$\mathcal{P}0 : \min_{\boldsymbol{x}, \boldsymbol{p}^{rf}, \boldsymbol{p}^{fso}} \sum_{i=1}^{N} x_i E_i^{rf} + (1-x_i)E_i^{fso} \quad (14a)$$

subject to:

$$\mathcal{C}_{0,1} : x_i T_i^{rf} + (1-x_i)T_i^{fso} \leq T_i^{max}, \forall i \quad (14b)$$

$$\mathcal{C}_{0,2} : x_i p_i^{rf} + (1-x_i)p_i^{fso} \leq p_i^{max}, \forall i \quad (14c)$$

$$\mathcal{C}_{0,3} : \sum_{i=1}^{N} x_i \leq K \quad (14d)$$

$$\mathcal{C}_{0,4} : x_i = \{0,1\}, \forall i \quad (14e)$$

In $\mathcal{P}0$, $\boldsymbol{x}$ denotes the vector of the link decision x_i, while $\boldsymbol{p}$ denotes the vector of the transmission power p_i. $\mathcal{C}_{0,1}$ enforces that the transmission time does not exceed the maximum tolerable latency, while $\mathcal{C}_{0,2}$ is employed to limit the total transmission power (i.e., p_i^{max}). Additionally, $\mathcal{C}_{0,3}$ limits the number of FSO links to the number of available optical receivers at the BS side. Finally, $\mathcal{C}_{0,4}$ forces binary values to x_i. $\mathcal{P}0$ is a non-convex non-linear problem due to the logarithms included in the throughput and $\mathcal{C}_{0,4}$ that makes the feasible set non-convex.

III. Proposed Solution

To solve the optimization problem, we develop a decomposition-driven algorithm [17], in which the link decision subproblem and power allocation subproblem are iteratively optimized. Particularly, the link decision subproblem is solved as an ILP problem, while the power allocation subproblem is solved by leveraging the Lagrange dual decomposition and subgradient methods [18].

A. Link Decision Subproblem

Assuming fixed power allocation, $\mathcal{P}0$ is reformulated as follows:

$$\mathcal{P}1 : \min_{\boldsymbol{x}} \sum_{i=1}^{N} x_i E_i^{rf} + (1-x_i)E_i^{fso} \quad (15a)$$

subject to:

$$\mathcal{C}_{1,1} : \sum_{i=1}^{N} x_i \leq K \quad (15b)$$

$$\mathcal{C}_{1,2} : x_i = \{0,1\}, \forall i \quad (15c)$$

$\mathcal{P}1$ is an ILP problem that can be solved using various methods, such as the branch-and-bound or interior-point methods, included in the CVX toolbox[1].

B. Power Allocation Subproblem

Assuming a fixed link decision vector, $\mathcal{P}0$ is reformulated as follows:

$$\mathcal{P}2 : \min_{\boldsymbol{p}^{rf}, \boldsymbol{p}^{fso}} \sum_{i=1}^{N} x_i E_i^{rf} + (1-x_i)E_i^{fso} \quad (16a)$$

subject to:

$$\mathcal{C}_{2,1} : x_i T_i^{rf} + (1-x_i)T_i^{fso} \leq T_i^{max}, \forall i \quad (16b)$$

$$\mathcal{C}_{2,2} : x_i p_i^{rf} + (1-x_i)p_i^{fso} \leq p_i^{max}, \forall i \quad (16c)$$

To solve $\mathcal{P}2$, we employ the Lagrange dual decomposition and subgradient methods. The Lagrangian of $\mathcal{P}2$ is obtained

[1] http://cvxr.com

Algorithm 1 Bisection Method for Finding the Optimal Power Allocation

Input: Maximum transmission power p_i^{max}

Output: Optimal p_i^*

Set $p_i^{LB} = 0$ and $p_i^{UB} = p_i^{max}$
repeat
  Set $X = \frac{p_i^{LB} + p_i^{UB}}{2}$
  if $\frac{\partial L}{\partial p_i} \cdot \frac{\partial L}{\partial p_i} < 0$ **then**
    $p_i^{UB} = X$
  else
    $p_i^{LB} = X$
  end if
until $|p_i^{UB} - p_i^{LB}| < 0.001$
Set $p_i^* = \frac{p_i^{LB} + p_i^{UB}}{2}$
Return p_i^*

by (5), shown at the top of the previous page. In (5), τ_i and π_i are the non-negative Lagrange multipliers. The dual function is written as

$$D(\tau_i, \pi_i) = \min_{p_i^{rf}, p_i^{fso}} \; L(p_i^{rf}, p_i^{fso}, \tau_i, \pi_i) \tag{17a}$$
$$\text{subject to:} \quad \mathcal{C}_{2,1}, \mathcal{C}_{2,2}$$

Consequently, the dual problem is expressed as

$$\max_{\tau_i, \pi_i} \; D(\tau_i, \pi_i) \tag{18a}$$
$$\text{subject to: } \tau_i \geq 0 \text{ and } \pi_i \geq 0, \forall i$$

In accordance to the Karush–Kuhn–Tucker (KKT) conditions, the derivatives of the Lagrangian with respect to p_i^{rf} and p_i^{fso} are obtained by (6) and (7), respectively. Since it is challenging to obtain closed-form expressions for both equations, we utilize to the bisection method (Algorithm 1) for finding the respective roots[2].

After obtaining the solution to the dual problem using (6), (7), and Algorithm 1, the Lagrange multipliers are updated as follows:

$$\tau_i^{t+1} = \left[\tau_i^t + s_1 \left(x_i \frac{L_i}{R_i^{rf}} + (1 - x_i) \frac{L_i}{R_i^{fso}} - T_i^{max} \right) \right]^+ \tag{19}$$

$$\pi_i^{t+1} = \left[\pi_i^t + s_2 \left(x_i p_i^{rf} + (1 - x_i) p_i^{fso} - p_i^{max} \right) \right]^+ \tag{20}$$

where t is the iteration number, while s_1 and s_2 are positive step sizes. The subgradient method for solving the dual problem is presented in Algorithm 2.

C. Overall Optimization Algorithm

Both problems $\mathcal{P}1$ and $\mathcal{P}2$ can be solved iteratively until convergence or reaching a pre-defined number of iterations as presented in Algorithm 3.

[2]Algorithm 1 is used for finding p_i^{rf} and p_i^{fso} by modifying the term ∂p_i accordingly.

Algorithm 2 Subgradient Method for Optimizing $\boldsymbol{p}^{rf}, \boldsymbol{p}^{fso}$

Input: Maximum transmission power $p_i^{max}, \forall i$

Output: Optimal $\boldsymbol{p}^{rf}, \boldsymbol{p}^{fso}$

Initialize $p_i^{rf} = p_i^{fso} = \frac{p_i^{max}}{2}, \forall i$
Initialize the Lagrange multipliers: $\tau_i, \pi_i, \forall i$
set $t = 0$
repeat
  for $i = 1$ **to** N **do**
    Calculate p_i^{rf} and p_i^{fso} using (6), (7), and Algorithm 1
    Update the Lagrange multipliers using (19) - (20)
  end for
  Set $\mathcal{E}[t] = \sum_{i=1}^{N} E_i(p_i^{rf}, p_i^{fso})$
  Set $t = t + 1$
until $|\mathcal{E}[t] - \mathcal{E}[t-1]| < 0.01$ or $t > 100$
Return $\boldsymbol{p}^{rf}, \boldsymbol{p}^{fso}$

Algorithm 3 Joint Link Selection and Power Allocation Algorithm for Solving $\mathcal{P}0$

Input: System parameters: $N, K, L_i, T_i^{max}, p_i^{max}, w_i^{rf}, w_i^{fso}$, $|h_i^{rf}|^2, |h_i^{fso}|^2, \forall i$

Output: Optimal $\boldsymbol{x}, \boldsymbol{p}^{rf}, \boldsymbol{p}^{fso}$

Set $l = 0$
repeat
  Find $x_i, \forall i$ by solving $\mathcal{P}1$ through CVX
  Find $p_i^{rf}, p_i^{fso}, \forall i$ by solving $\mathcal{P}2$ using Algorithm 2
  Set $\mathcal{E}[l] = \sum_{i=1}^{N} E_i(x_i, p_i^{rf}, p_i^{fso})$
  if $\mathcal{E}[l] < \mathcal{E}^*$ **then**
    Set $x_i^* = x_i, p_i^{rf*} = p_i^{rf}, p_i^{fso*} = p_i^{fso}, \forall i$
  end if
  Set $l = l + 1$
until $|\mathcal{E}[t] - \mathcal{E}[t-1]| < 0.01$ or $l > 100$
Return $\boldsymbol{x}, \boldsymbol{p}^{rf}, \boldsymbol{p}^{fso}$

IV. Performance Evaluation

To evaluate the performance of our proposed algorithm, we utilize Monte Carlo simulations. Specifically, we evaluate the total energy consumption of the system with respect to the number of devices and the available RF/FSO bandwidth. The IIoT devices are randomly distributed in the coverage area of the BS, while their distances from the BS are in the range of $[0, 500]$ m. The number of IIoT devices ranges from 2 to 30, while the task size of each device is in the range of $[0.5, 3]$ Mbits and the delay tolerance is set to 1 second. Also, the available power budget of each device is set to 5 watts. Moreover, the number of the BS FSO transceivers ranges from 2 to 10, the total available bandwidth of the RF and FSO

links are respectively set to $\{1, 5, 10\}$ MHz, and each FSO link wavelength is $\lambda = 1550$ nm. Finally, a clear weather environment is assumed (i.e., $\alpha = 0.96$), the FSO transmitter and receiver aperture diameters are 0.1 m, while the step sizes for the Lagrange multiplier updates are set to $s_1 = s_2 = 0.1$. The final results are generated by averaging 500 Monte Carlo simulations. The simulation parameters are summarized in Table I.

TABLE I
SIMULATION PARAMETERS

Parameter	**Value**
Number of devices	2–30
Distance between the BS and the devices	$[0, 500]$ m
Number of FSO transeivers at the BS	2–10
FSO transceiver aperture diameter	0.1 m
Task size	$[0.5, 3]$ Mbits
Power budget	5 Watts
Task delay tolerance	1 s
RF and FSO bandwidth	1, 5, 10 MHz
FSO wavelength	1550 nm
Weather coefficient	0.96
Step sizes	0.1

The total energy consumption as a function of the number of devices for various FSO transceivers is presented in Fig. 2. Particularly, the number of devices ranges from 2 to 30, while the number of FSO transceivers in the BS ranges from 2 to 10. Moreover, the available bandwidth for both RF and FSO links is set to 1 MHz. As the number of devices is increased the total energy consumption is also increased. This is expected as there exist more devices in the network. Additionally, when the number of FSO transceivers is increased the total energy consumption is decreased, since the FSO communications can achieve high capacity links with lower power consumption compared to RF communications.

The total energy consumption as a function of the RF bandwidth for various FSO bandwidth settings is depicted in Fig. 3. For both RF and FSO links, the available bandwidth is set to 1, 5, and 10 MHz, while the numbers of devices and FSO transceivers are set to 20 and 10, respectively. When the available RF bandwidth is increased, the energy consumption is decreased as lower power levels are required for the timely uploading of each task. The same applies to the FSO bandwidth since more available bandwidth can lead to higher capacity FSO links.

Finally, the convergence over the course of iterations for various devices and transceivers configurations is shown in Fig. 4. When the number of devices is 30, the initial energy consumption of the system is high, since the maximum available power has been allocated to each device. Consequently, fewer devices result in lower initial energy consumption. Moreover, in the

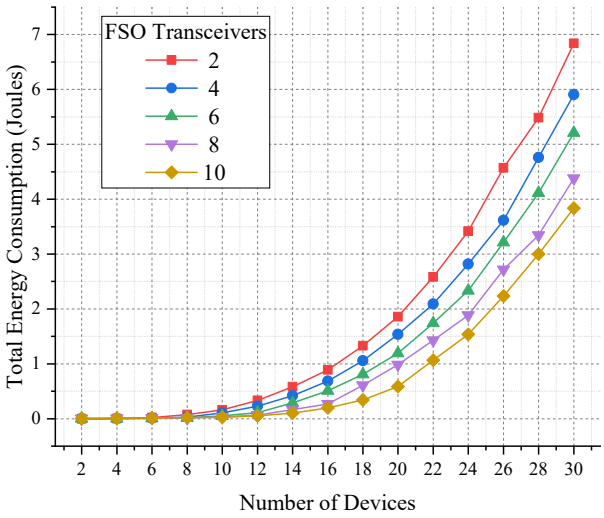

Fig. 2. Total energy consumption as a function of the number of devices for various numbers of FSO transceivers

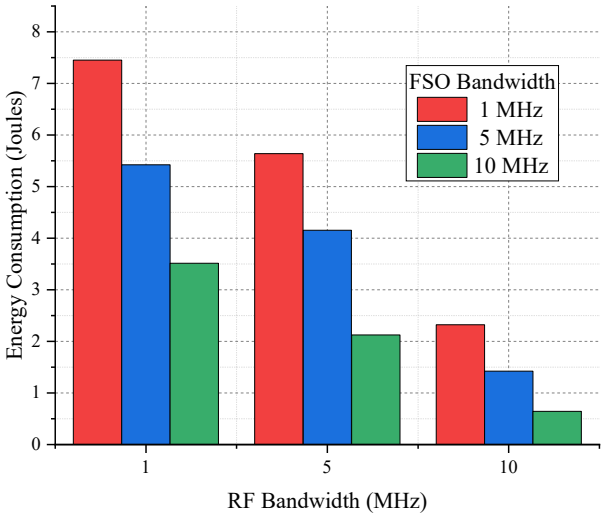

Fig. 3. Total energy consumption as a function of the RF bandwidth for various FSO bandwidth configurations

case of 30 devices, the proposed solution converges after 15 iterations. On the other hand, when the number of devices is 5, the solution converges after 5 iterations.

V. CONCLUSION

In this work, we presented a hybrid RF-FSO system to support the task offloading process in IIoT environments and developed a solution that minimizes the total energy consumption of the system by deciding whether the RF or FSO link will be used for the task offloading and optimally allocating the device transmission power. Due to the complexity of the initial optimization problem, we decoupled it into two problems that were iteratively solved until convergence. Specifically, the RF-FSO link decision subproblem was solved using the CVX toolbox with the Mosek solver, while the

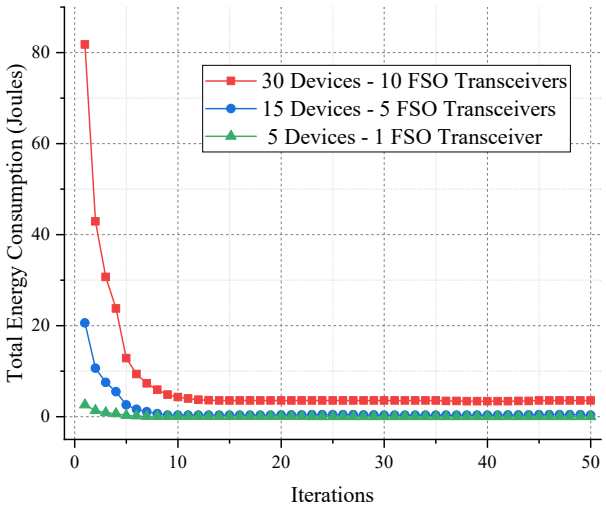

Fig. 4. Convergence over the course of iterations for various device and transeciver configurations

power optimization subproblem was solved by leveraging the Lagrange dual decomposition and subgradient methods.

To validate our proposed solution, we carried out system-level Monte Carlo simulations and evaluated the system energy consumption with respect to the number of devices and the available RF/FSO bandwidth. The simulation results show that the proposed solution can minimize the total energy consumption of the system while taking into account the task requirements in terms of delay.

As future work, we aim to extend this scenario by including IoT devices that are far from the BS coverage region and are not equipped with FSO transceivers. In this direction, UAVs equipped with FSO transceivers can form wireless local area networks and act as relays between the IoT devices and the BS [19]. Due to the limited energy reserves, the position and transmission power of the UAVs have to be carefully specified [20], [21]. Furthermore, schemes that facilitate the accommodation of massives numbers of IoT devices can be leveraged [22], [23]. Finally, we aim to investigate the concurrent use of both FSO and RF transceivers to upload a device task.

Acknowledgment

This work has received funding from the European Union's Horizon 2020 research and innovation programme under grant agreement No. 957406 (TERMINET).

References

[1] C. D. Alwis, A. Kalla, Q.-V. Pham, P. Kumar, K. Dev, W.-J. Hwang, and M. Liyanage, "Survey on 6G frontiers: Trends, applications, requirements, technologies and future research," *IEEE Open Journal of the Communications Society*, vol. 2, pp. 836–886, 2021.

[2] M. Giordani, M. Polese, M. Mezzavilla, S. Rangan, and M. Zorzi, "Toward 6G networks: Use cases and technologies," *IEEE Communications Magazine*, vol. 58, no. 3, pp. 55–61, Mar. 2020.

[3] M. Z. Chowdhury, M. Shahjalal, S. Ahmed, and Y. M. Jang, "6G wireless communication systems: Applications, requirements, technologies, challenges, and research directions," *IEEE Open Journal of the Communications Society*, vol. 1, pp. 957–975, 2020.

[4] N. Chen and M. Okada, "Toward 6G internet of things and the convergence with RoF system," *IEEE Internet of Things Journal*, vol. 8, no. 11, pp. 8719–8733, Jun. 2021.

[5] Y. Kaymak, R. Rojas-Cessa, J. Feng, N. Ansari, M. Zhou, and T. Zhang, "A survey on acquisition, tracking, and pointing mechanisms for mobile free-space optical communications," *IEEE Communications Surveys & Tutorials*, vol. 20, no. 2, pp. 1104–1123, 2018.

[6] M. A. Khalighi and M. Uysal, "Survey on free space optical communication: A communication theory perspective," *IEEE Communications Surveys & Tutorials*, vol. 16, no. 4, pp. 2231–2258, 2014.

[7] A. Douik, H. Dahrouj, T. Y. Al-Naffouri, and M.-S. Alouini, "Hybrid radio/free-space optical design for next generation backhaul systems," *IEEE Transactions on Communications*, vol. 64, no. 6, pp. 2563–2577, Jun. 2016.

[8] M. N. Khan and M. Jamil, "Adaptive hybrid free space optical/radio frequency communication system," *Telecommunication Systems*, vol. 65, no. 1, pp. 117–126, Aug. 2016.

[9] M. N. Khan, S. O. Gilani, M. Jamil, A. Rafay, Q. Awais, B. A. Khawaja, M. Uzair, and A. W. Malik, "Maximizing throughput of hybrid FSO-RF communication system: An algorithm," *IEEE Access*, vol. 6, pp. 30 039–30 048, 2018.

[10] J.-H. Lee, K.-H. Park, M.-S. Alouini, and Y.-C. Ko, "Free space optical communication on UAV-assisted backhaul networks: Optimization for service time," in *2019 IEEE Globecom Workshops (GC Wkshps)*, 2019, pp. 1–6.

[11] M. Najafi, V. Jamali, D. W. K. Ng, and R. Schober, "C-RAN with hybrid RF/FSO fronthaul links: Joint optimization of fronthaul compression and RF time allocation," *IEEE Transactions on Communications*, vol. 67, no. 12, pp. 8678–8695, 2019.

[12] H. Safi, A. Dargahi, J. Cheng, and M. Safari, "Analytical channel model and link design optimization for ground-to-hap free-space optical communications," *J. Lightwave Technol.*, vol. 38, no. 18, pp. 5036–5047, Sep. 2020.

[13] M. S. Bashir and M.-S. Alouini, "Optimal power allocation between beam tracking and symbol detection channels in a free-space optical communications receiver," *IEEE Transactions on Communications*, vol. 69, no. 11, pp. 7631–7646, 2021.

[14] Y. Li, T. Geng, R. Tian, and S. Gao, "Power allocation in a spatial multiplexing free-space optical system with reinforcement learning," *Optics Communications*, vol. 488, p. 126856, 2021.

[15] M. Alzenad, M. Z. Shakir, H. Yanikomeroglu, and M.-S. Alouini, "FSO-based vertical backhaul/fronthaul framework for 5G+ wireless networks," *IEEE Communications Magazine*, vol. 56, no. 1, pp. 218–224, 2018.

[16] M. Safari, M. M. Rad, and M. Uysal, "Multi-hop relaying over the atmospheric poisson channel: Outage analysis and optimization," *IEEE Transactions on Communications*, vol. 60, no. 3, pp. 817–829, Mar. 2012.

[17] L. Liu, B. Sun, X. Tan, and D. H. K. Tsang, "Energy-efficient resource allocation and subchannel assignment for NOMA-enabled multiaccess edge computing," *IEEE Systems Journal*, pp. 1–12, 2021.

[18] L. V. Stephen Boyd, *Convex Optimization*. Cambridge University Press, Mar. 2004.

[19] T. Lagkas, G. Papadimitriou, P. Nicopolitidis, and A. Pomportsis, "A new approach to the design of MAC protocols for wireless LANs: combining QoS guarantee with power saving," *IEEE Communications Letters*, vol. 10, no. 7, pp. 537–539, Jul. 2006.

[20] D. Pliatsios, P. Sarigiannidis, S. K. Goudos, and K. Psannis, "3D placement of drone-mounted remote radio head for minimum transmission power under connectivity constraints," *IEEE Access*, vol. 8, pp. 200 338–200 350, 2020.

[21] X. Jiang, Z. Wu, Z. Yin, Z. Yang, and N. Zhao, "Power consumption minimization of UAV relay in NOMA networks," *IEEE Wireless Communications Letters*, vol. 9, no. 5, pp. 666–670, 2020.

[22] D. Pliatsios, A.-A. A. Boulogeorgos, T. Lagkas, V. Argyriou, I. D. Moscholios, and P. Sarigiannidis, "Semi-grant-free non-orthogonal multiple access for tactile internet of things," in *2021 IEEE 32nd Annual International Symposium on Personal, Indoor and Mobile Radio Communications (PIMRC)*. IEEE, Sep. 2021.

[23] T. D. Lagkas, D. G. Stratogiannis, and P. Chatzimisios, "Modeling and performance analysis of an alternative to IEEE 802.11e hybrid control function," *Telecommunication Systems*, vol. 52, no. 4, pp. 1961–1976, Jun. 2011.